J Mater Sci: Mater Med (2010) 21:1489–1494
DOI 10.1007/s10856-010-3999-3

Biomimetic whisker-shaped apatite coating of titanium powder

**Young Uk Sim · Jong Hee Kim · Tae Young Yang ·
Seog Young Yoon · Hong Chae Park**

Received: 23 September 2009 / Accepted: 9 January 2010 / Published online: 22 January 2010

Abstract Biomimetic apatite coatings on chemically modified titanium powder have been processed and the resulting coating layers evaluated in terms of morphology, composition and structure, using TF-XRD, XPS, SEM, TEM and FTIR analysis. After 7 days immersion in a simulated body fluid (SBF), nanometer-sized fine precipitates with an amorphous whisker-like phase and a Ca/P atomic ratio of 1.94 were obtained on the external surface of the titanium particles. When the immersion time in SBF was extended to 16 days, the coating layer consisted of the whisker-like nanostructured crystals of carbonated hydroxyapatite with a atomic ratio of 3; in such a case, a double coating layer was developed. The double layer could be divided into two regions and could be clearly distinguished: an inner dense region ($\sim$200 nm in thickness) which may include hard agglomerated crystals and an outer less dense region ($>$ 500 nm in thickness) in which crystals are loosely distributed.

1 Introduction

Titanium and its alloys such as Ti6Al4V have been widely used for implant fabrication both in dentistry and surgery because of their good mechanical properties, biocompatibility and corrosion resistance [1, 2]. However, such metals are bioinert, and do not easily bond directly to the bone. Apatite is a bioactive ceramic, this allowing good osteoconductivity [3]. Unfortunately, the bioactive ceramic exhibits poor mechanical properties; consequently it is not suitable for load-bearing biomedical applications [4]. A bioactive coating of titanium and its alloys can combine the osteoconductivity of apatite with the mechanical properties of a metal. Various processing routes for preparing bioactive ceramic coatings on titanium and its alloys have been reported including plasma spraying [5–9], the sol–gel method [10, 11], electrophoresis and electrochemical deposition [12, 13]. Among these processing methods, the plasma spraying technique is often used for hydroxyapatite (HA) coating of metal implants owing to its high deposition rate and ability to coat a wide area; however, it needs a very high deposition temperature, this undesirably resulting in the partial decomposition of HA [5]. Further, the plasma coating exhibits poor adhesion strength between the HA coating and the substrate, inhomogeneous coating quality and unsuitability for the coating of complex-shaped implants [14].

On the other hand, a biomimetic deposition technique [15–18], using an acellular simulated body fluid (SBF) has attracted much attention, in that it describes the formation of a bone-like apatite surface layer on a titanium substrate. The apatite nucleates on the surfaces of chemically treated titanium in SBF and grows continuously by consuming calcium and phosphate ions from the surrounding fluid to form uniform apatite layer. Up to now, almost all researches on the biomimetic apatite coatings have been carried out with a flat-shaped titanium substrate. In the present work, a biomimetic processing route for nanostructured whisker-shaped apatite coatings on titanium powder has been proposed and the resulting coating material characterized. It is expected that such apatite-coating titanium powder may exhibit the strength of the metal together with the bioactivity of the ceramic; consequently, it offers the potential to be used as a promising candidate material for a

---

Y. U. Sim · J. H. Kim · T. Y. Yang · S. Y. Yoon ·
H. C. Park (✉)
School of Materials Science and Engineering, Pusan National University, Pusan 609-735, South Korea
e-mail: hcpark1@pusan.ac.kr

variety of biomedical applications such as bone filler, dental repair, and artificial scaffold.

2 Materials and methods

Commercial-grade titanium powder (Sigma–Aldrich Co.) with a purity of 99.75% and an agglomerate size of 41.46 μm was used in this investigation. After ultrasonically washing with ethanol and deionized water, and drying at 50°C, the titanium powder was etched in 3 M HCl at 60°C for 1 h, soaked in 5 M NaOH aqueous solution at 60°C for 24 h, filtered, washed with distilled water and dried at 100°C for 2 h.

The chemically treated titanium powder was soaked for 3–16 days at 36.5°C in SBF with the ion concentrations (mM) of 142.0 Na^+, 5.0 K^+, 1.5 Mg^{2+}, 2.5 Ca^{2+}, 148.8 Cl^-, 4.2 HCO^{3-}, 1.0 $HPO_4{}^{2-}$ and 0.5 $SO_4{}^{2-}$. The solution was prepared by dissolving reagent-grade NaCl, $NaHCO_3$, KCl, $K_2HPO{\cdot}3H_2O$, $MgCl_2{\cdot}6H_2O$, $CaCl_2$ and Na_2SO_4 in distilled water. It was buffered at pH = 7.4 with tris-hydroxymethyl aminomethane (TRIS) and HCl at 36.5°C.

The coating layer developed on the titanium powder was examined by scanning electron microscopy (SEM, S-4200, Hitachi) at 15 kV and transmission electron microscopy (TEM, JEM-2010, Jeol) at 200 kV to determine the surface morphology. The thickness of coating layer was approximately determined from TEM micrographs. The chemical and crystalline phase compositions were investigated by Fourier transform infrared reflection spectroscopy (FTIR, IFS-66, Bruker) and thin-film X-ray diffractometry (TF-XRD, D/MAX 2200, Rigaku) at a glancing angle of 1°. The elemental composition and surface chemistry were examined using energy dispersive X-ray microanalysis (EDX, 6853-H, Horiba) and X-ray photoelectron spectroscopy (XPS, ESCALAB 250, VG Scientific). The binding energies measured in XPS were calibrated relative to the hydrocarbon C1s of 284.6 eV.

3 Results and discussion

After immersing the chemically modified titanium powder in SBF, the surface microstructures of the coating layers are shown in Fig. 1. With increasing immersion time, up to 5 days, the surface structure of the titanium powder was loosened, probably due to the dissolution of Na^+ ions from the surface of the titanium powder via exchange with H_3O^+ ions in SBF. A clear trace of the reaction products could not be seen. When immersed for 7 days, however, nanometer-sized fine precipitates formed in a large volume on the surfaces of the titanium particles (Fig. 1c). With the extension of the immersion time to 16 days, a relatively large number of whisker-like crystals were developed (Fig. 1d). Their morphology could be clearly distinguished from the reaction products deposited from SBF on a planar titanium substrate, typically isolated spheroidal particles [19–21].

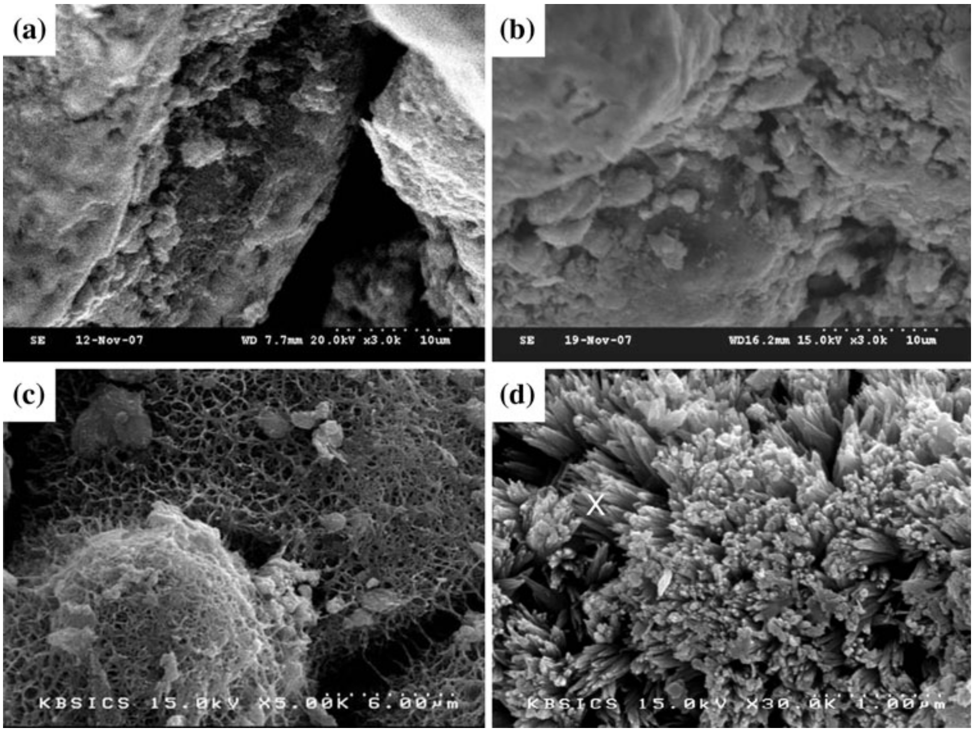

Fig. 1 SEM micrographs of the surfaces of chemically modified titanium powder after immersing in SBF for **a** 3, **b** 5, **c** 7 and **d** 16 days

Development of the whisker-like phase in the particulate titanium substrate depends on the presence of nucleation sites and the presence of a sufficient concentration of ionic species necessary to form the apatite. Growth of the whiskers is possibly due to the following:

i. relatively high specific surface area of the rugged titanium particles which provides nucleation sites for apatite in SBF at the sharp edges and peaks of the surface compared with planar substrates, results in more energetic nucleation sites
ii. when a nucleus forms on a particulate titanium substrate, the contact area between substrate and nucleus is small enough such that a preferred orientation growth habit is active
iii. the ions necessary for growth can diffuse to the nucleation site from many directions; in comparison with the planar surface, the particulate surface can provide many nucleation sites and a linear diffusion path, perpendicular to the plane of the substrate, for the ionic species necessary for growth; the apatite thus grows into a whisker-like phase rather than becoming spherical
iv. the crystal structure has a hexagonal unit cell ($a = 0.941$ nm, $c = 0.689$ nm), allowing preferential crystal growth along the crystallographic direction parallel to the *c*-axis compared with any other direction.

After immersing in SBF for 7 and 16 days, the morphologies of the surfaces of coating layers were observed in detail by TEM (Fig. 2). With an immersion time of 7 days, the coating layer with the thickness of <200 nm (Fig. 2a) consisted of a nanostructured whisker-like phase. This is believed to be amorphous from the evidence of selected area diffraction (SAD) patterns. After immersion for 16 days, the whisker-like phase illustrated in Fig. 1d exhibited three microstructural features having different morphology: whisker-shaped, rod-shaped and polygonal-shaped crystals all with a nano dimensions. As shown in Fig. 2b, in such cases, besides the dense coating layer (~200 nm in thickness) on the surface of the titanium particles, the nanostructured and agglomerated crystals were also present at even further distances from the interface of the coating layer and were somewhat loosely connected to each other. The presence of this complex coating layer could suggest that further nucleation of the precipitates in SBF solution may be associated with nanoparticles which had already been precipitated on the external surface of the titanium, subsequently these being able to act as nucleation seeds. It is expected that when implanted the loosely connected fine crystals could easily be redissolved and increase the degree of supersaturation near the surface of the dense coating, contributing positively to further improved formation and growth of the bone.

The TF-XRD patterns of the surface of the titanium powder immersed in SBF for 7 and 16 days are shown in Fig. 3. Titanium and rutile phases were identified after immersion for 7 days; the presence of apatite crystals was not observed. After immersion for 16 days however, the characteristic peaks of carbonated hydroxyapatite (CHA) with Miller indices of (0 0 2), (1 1 2), (3 0 0) (JCPDS Card #19-0272) were detected, but the peak intensities were relatively low compared with titanium and rutile. It is proposed that nanometer-sized crystals with a low

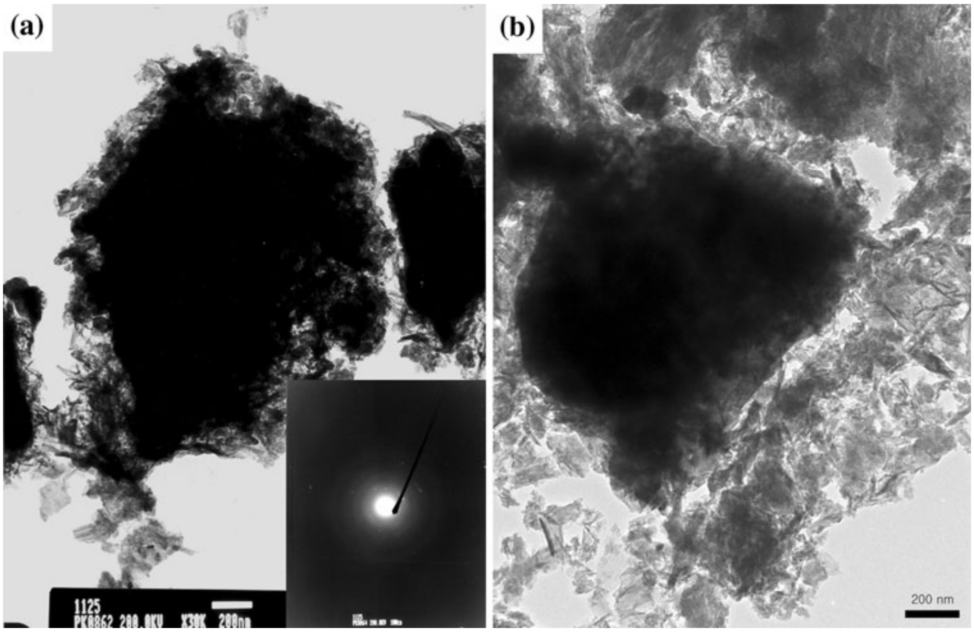

Fig. 2 TEM micrographs of the surface of the titanium powder after immersing in SBF for **a** 7 and **b** 16 days

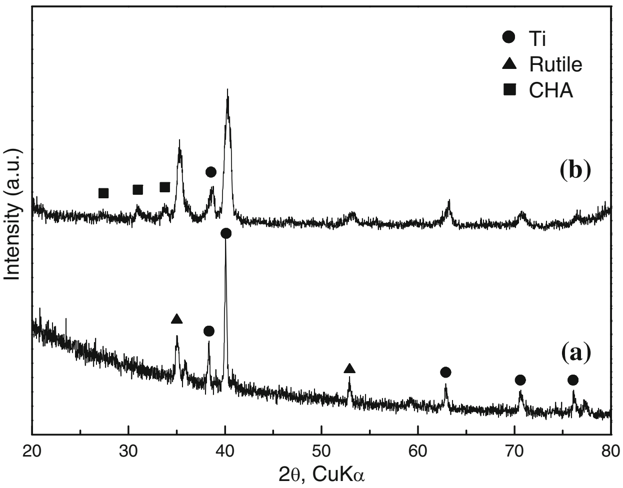

Fig. 3 TF-XRD patterns of the titanium powder after immersing in SBF for **a** 7 and **b** 16 days

crystallinity were developed on the surfaces of the titanium particles, as shown in Fig. 2.

As shown in Fig. 4, EDX analysis revealed the presence of carbon, oxygen, sodium (or magnesium) and phosphorus in the surface of titanium powder immersed in SBF, in which the major chemical components of calcium phosphate compounds were contained. It is considered that minor amounts of sodium remain in spite of washing with distilled water after alkali treatment and in the initial reaction stage, the Mg^{2+} ions are incorporated with Ca^{2+} on the surface of the titanium powder. After immersing for 7 days in SBF, the Ca/P atomic ratio was 1.94, determined by EDX area analysis. After 16 days, the Ca/P atomic ratio increased to 3 when determined by EDX point analysis on a spot ('marked 'X' in Fig. 1d) on the whisker-shaped particle, which is further close to the stoichiometric composition (3.3, atomic ratio) of CHA ($Ca_{10}(PO_4)_3(CO_3)_3(OH)_2$, JCPDS card # 19-0272). Thus in the development of the biomimetic reaction of the titanium powder, the bone-like apatite crystals appear to be formed via intermediate products of calcium phosphate [21].

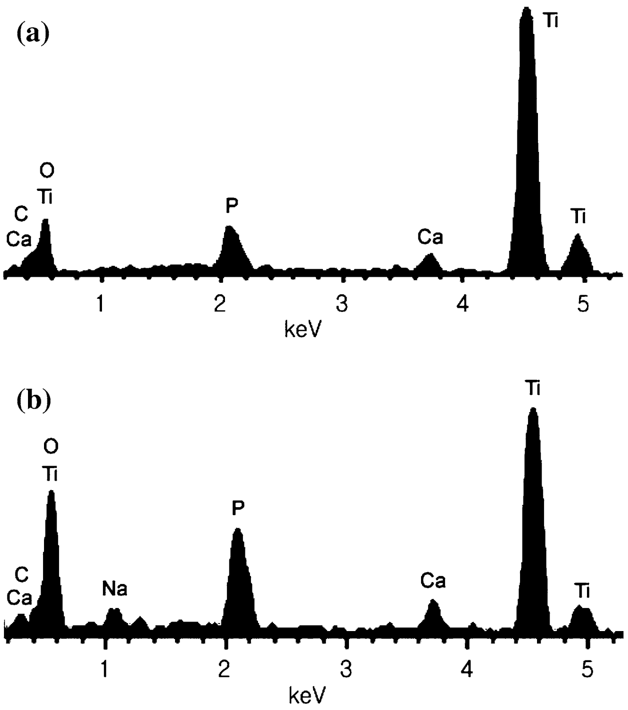

Fig. 4 EDX spectra of the surfaces of the titanium powder immersed in SBF for **a** 7 and **b** 16 days. Full scale: **a** 920 and **b** 768 cts

The XPS spectra of the titanium powder immersed in SBF for 16 days are shown in Fig. 5. C, Ca, O, P, and Ti were detected on the surface of the coating layer. The binding energies (BE) of $Ti2p_{3/2}$ and $Ti2p_{1/2}$ were detected at 458.4 and 463.8 eV, respectively, corresponding to a quadrivalent oxidation state (Ti^{4+}) (Fig. 5b) [22]. The BE values coincide with those typical for TiO_2, the chemical composition of rutile subsequently confirmed by TF-XRD analysis (Fig. 3). It is assumed that the presence of TiO_2 is due to the residual passive oxide film that was not removed by etching in HCl ($TiO_2 + 4HCl \rightarrow TiCl_4 + 2H_2O$) and/or subsequently soaking in NaOH ($TiO_2 + NaOH \rightarrow HTiO_3 + Na^+$) [21]. The oxide film could also have grown rapidly by oxidation at room temperature after the cleaning process and before immersion in the SBF. The Ca2p spectrum exhibited a doublet with $Ca2p_{3/2}$ (346.4) and $Ca2p_{1/2}$ (349.9 eV) (Fig. 5c), corresponding to Ca^{2+} [23]. The P2p spectrum showed a single peak at 133.0 eV ($P2p_{3/2}$) (Fig. 5d), corresponding to P^{5+}. These BE values of Ca2p and P2p were very similar to those of CHA, reported in the published literature [22–24]. Also, the FTIR absorption bands shown in Fig. 6 were fundamentally in agreement with the characteristic absorption bands for H_2O, PO_4^{3-} and CO_3^{2-} groups of CHA coating material reported in the literature [24]. Additionally, HPO_4^{2-} and OH^- bands were confirmed at 865 and 634 cm^{-1}, respectively, which would infer a slight calcium deficiency induced in SBF ($PO_4^{3-} + H_2O = HPO_4^{2-} + OH^-$) [25].

4 Conclusions

Nanostructured, whisker-shaped apatite coatings of chemically treated titanium powder have been prepared by a biomimetic growth process. The phase, composition and morphological development of the whiskers in the coating can be controlled using immersion time in SBF. After immersing in SBF for 7 days, nanometer-sized fine precipitates formed in large volumes on the external surface of titanium particles. These were shown to be an amorphous phase with a Ca/P atomic ratio of 1.94. With increasing in the immersion time to 16 days, the precipitates became

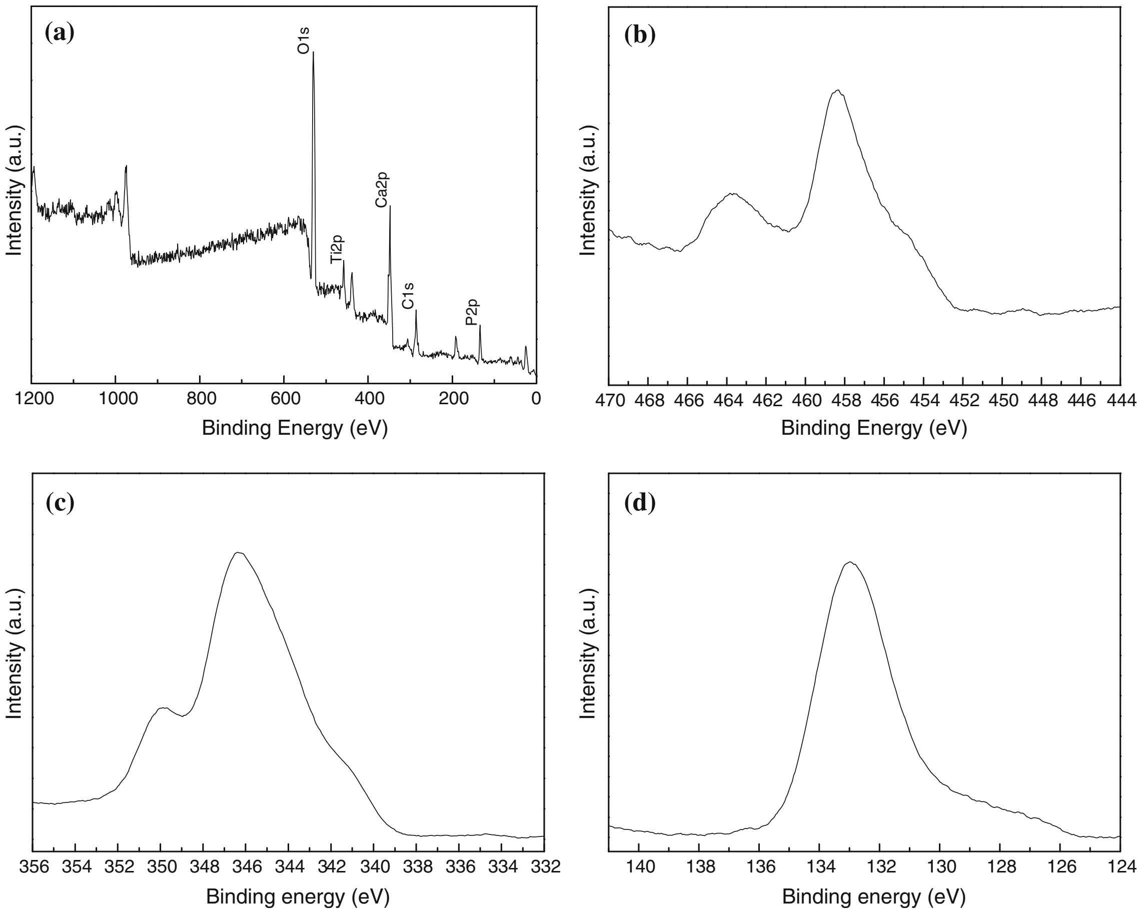

Fig. 5 XPS spectra of **a** XPS survey, **b** Ti2p, **c** Ca2p, and **d** P2p of the surface of the titanium powder immersed in SBF for 16 days

Fig. 6 FTIR spectrum of the titanium powder after immersing in SBF for 16 days

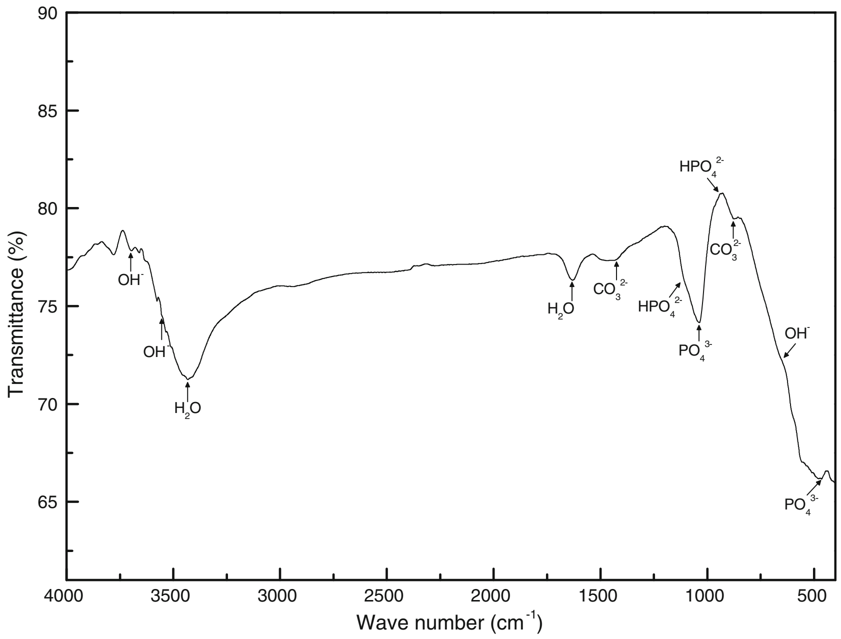

nanocrystalline whisker-like carbonated hydroxyapatite with a Ca/P atomic ratio of 3, close to the corresponding stoichiometric composition. The coating layer obtained after immersion for 16 days consisted of an inner dense region and an outer loose region of apatite crystals; the layer thickness in the latter appeared to be more than a double that in the former (about 200 nm), due to loosely packed particles.

Acknowledgements This work was supported by National Research Foundation of Korea Grant funded by the Korea Government (2009-0070577).

References

1. Long M, Rack HJ. Titanium alloy in total joint replacement—a materials science perspective. Biomaterials. 1998;19:1621–39.
2. Liu XY, Paul KC, Ding CX. Surface modification of titanium, titanium alloys, and related materials for biomedical applications. Mater Sci Eng R. 2004;47:49–121.
3. Wang M. Developing bioactive composite materials for tissue replacement. Biomaterials. 2003;24:2133–51.
4. Jose MG-V, Eduardo S, Antoni PT, Takeo O, Katsuaki S, Grayson WM, et al. Novel bioactive functionally graded coatings on Ti6Al4V. Adv Mater. 2000;12:894–9.
5. Feng CF, Khor KA, Liu EJ, Cheang P. Phase transformations in plasma sprayed hydroxyapatite coatings. Scripta Mater. 2000;42: 103–9.
6. Zheng XB, Huang MH, Ding CX. Bond strength of plasma-sprayed hydroxyapatite/Ti composite coatings. Biomaterials. 2000;21: 841–9.
7. de Groot K, Geesink R, Klein CPAT, Serekian P. Plasma sprayed coatings of hydroxyapatite. J Biomed Mater Res. 1987;21:1375–81.
8. Thomas KA, Kay JF, Cook SD, Jarcho M. The effect of surface macrotexture and hydroxyapatite coating on the mechanical strength and histological profiles of titanium implant materials. J Biomed Mater Res. 1987;21:1395–414.
9. Klein CPAT, Patka P, van der Lubbe HBM, Wolke JGC, de Groot K. Plasma-sprayed coatings of tetracalciumphosphate, hydroxy-apatite, and α-TCP on titanium alloy: an interface study. J Biomed Mater Res. 1991;25:53–65.
10. Hsieh MF, Perng LH, Chin TS. Hydroxyapatite coating on Ti6Al4V alloy using a sol-gel derived precursor. Mater Chem Phys. 2002;74:245–50.
11. Milella E, Cosentino F, Licciulli A, Massaro C. Preparation and characterisation of titania/hydroxyapatite composite coatings obtained by sol-gel process. Biomaterials. 2001;22:1425–31.
12. Cheng XL, Filiagg M, Roscoe SG. Electrochemically assisted co-precipitation of protein with calcium phosphate coatings on titanium alloy. Biomaterials. 2004;25:5395–403.
13. Shirkhanzadeh M. Calcium phosphate coatings prepared by electrocrystallization from aqueous electrolytes. J Mater Sci Mater Med. 1995;6:90–3.
14. de Groot K, Wen HB, Liu Y, Layrolle P, Barrere F. Biomimetic coatings on orthopedic implants: a review. In: Li P, Calvert P, Kokubo T, Levy R, Scheid C, editors. Mineralization in natural and synthetic biomaterials. Warrendale, PA: Materials Research Society; 2000. p. 109–16.
15. Kokubo T, Kushitani H, Sakka S, Kitsugi T, Yamamuro T. Solutions able to reproduce in vivo surface-structure changes in bioactive glass-ceramics A-W. J Biomed Mater Res. 1990;24: 721–34.
16. Takadama H, Kim HM, Kokubo T, Nakamura T. TEM-EDX study of mechanism of bone-like apatite formation on bioactive titanium metal in simulated body fluid. J Biomed Mater Res. 2001; 57: 441–8.
17. Kokubo T, Miyaji F, Kim HM, Nakamura T. Spontaneous formation of bonelike apatite layer on chemically treated titanium metals. J Am Ceram Soc. 1996;79:1127–9.
18. Kokubo T. Formation of biologically active bone-like apatite on metals and polymers by a biomimetic process. Thermochim Acta. 1996;280(/281):479–90.
19. Kim HM. Bioactive ceramics: challenges and perspectives. J Ceram Soc Jap. 2001;109:S49–57.
20. Kokubo T, Kim HM, Kawashita M, Nakamura T. Novel ceramics for biomedical applications. J Aust Ceram Soc. 2000;36:37–46.
21. Jonášová L, Műller FA, Helebrant A, Strnad J, Greil P. Biomimetic apatite formation on chemically treated titanium. Biomaterials. 2004;25:1187–94.
22. Frauchiger VM, Schlottig F, Gasser B, Textor M. Anodic plasma-chemical treatment of CP titanium surfaces for biomedical applications. Biomaterials. 2004;25:593–606.
23. Song WH, Jun YK, Han Y, Hong SH. Biomimetic apatite coating on micro-arc oxidized titania. Biomaterials. 2004;25:3341–9.
24. Wei D, Zhou Y, Jia D, Wang Y. Biomimetic apatite deposited on microarc oxidized anatase-based ceramic coating. Ceram Inter. 2008;34:1139–44.
25. Monma H, Kanazawa T. The hydration of α-tricalcium phosphate. J Ceram Soc Jpn. 1976;84:209–13.